Proceedings of the ASME 2021 40th International
Conference on Ocean, Offshore and Arctic Engineering
OMAE2021
June 21-30, 2021, Virtual, Online

OMAE2021-60529

AUTOMATED PATTERN RECOGNITION IN REAL-TIME DRILLING DATA FOR EARLY KARST DETECTION

Danil Maksimov[1], **Marius Alexander Løken**[1], **Alexey Pavlov**[1], **Sigbjørn Sangesland**[1]
[1]Norges teknisk-naturvitenskapelige universitet - NTNU, Trondheim, Norway

ABSTRACT

Drilling in carbonate formations often poses a real challenge to operators, contractors and service companies. Severe fluid losses, gas kicks and other unwanted situations increase drilling risks. These risks are closely related to drilling through karsts - vugs, cavities and fractures. Therefore it is important to detect karsts early enough to avoid drilling into them or, once drilling in a karstification region is detected, to prepare risk mitigating actions. Some geophysical methods can be used for karsts detection, however, they have limitations and cannot guarantee early detection of karsts. One of the recent studies has shown that certain patterns in real-time drilling data can serve as indicators of zones with a higher likelihood of encountering karsts. In this paper, we demonstrate how these patterns can be detected in an automated manner with an adaptive differential filter algorithm. The method has been validated on real drilling data.

NOMENCLATURE

ADF Adaptive Differentiating Filter
BHA Bottom Hole Assembly
LCM Lost Circulation Material
LWD Logging While Drilling
PLA Piecewise Linear Approximation
PMCD Pressurized Mud Cap Drlling
RCD Rotational Control Device
ROP Rate Of Penetration
SPP Stand Pipe Pressure
WOB Weight On Bit
WR Window Radius

1 INTRODUCTION

Carbonate reservoirs are the most important sources of the world's oil and gas production [1]. The highest production rates from carbonate reservoirs are commonly associated with multiple-porosity systems and can generally be classified into depositional (primary) and post-depositional (secondary pores). On the one hand, such dual-porosity of carbonates makes them a valuable geological target. On the other hand, the appearance of secondary porosity is a direct consequence of dissolution of soluble rocks [2] - the process that not only results in the development of high-porosity reservoirs, but also contributes to the development of vugs, enlarged fractures and caves [3]. These, are known as karsts [4,5]. They can be found at different depths [6] and they can be both - collapsed or not-collapsed.

Drilling through karsts can be equally dangerous, potentially expensive and time consuming. Lost circulation of drilling fluid and gas kicks often accompany drilling in such intervals. Shell has reported that every sixth well drilling in carbonates in Sarawak, Peninsular Malaysia, resulted in total losses (Sarawak, Peninsular Malaysia) [7]. In Qatar a "large volume of cement" was pumped during few weeks to plug intervals of mud losses in carbonates [8]. Similar problems exist on the Norwegian Continental Shelf, when drilling into karsts resulted in total losses during a week [9–11].

Mitigation of these problems by adding Lost Circlation Material (LCM) may give only a short-term effect and cannot help when big karsts need to be plugged [12]. The use of Pressurized Mud Cap Drilling (PMCD), when a sacrificial fluid is pumped through the bit nozzles to fill karsts, is today the most common solution to dealing with total losses in carbonates [13–15]. However, rigs are not always equipped with a Rotational Control De-

vice (RCD) [16] required for PMCD and a significant volume of sacrificial drilling fluid may not be readily available.

Prediction and/or early detection of zones with high likelihood of karstification is important for drilling safety, as it allows one to prepare risk mitigating actions early. Such prediction is not a trivial task as even with the cutting-edge geophysical methods it is still challenging to detect karsts. For example, it was shown that conventional seismic methods cannot detect caves less than $\frac{\lambda}{4}$ (40 m) due to wave interference [17]. Based on the experience of drilling in the Barents Sea, where the average size of caves is less than a meter, we can conclude that even such relatively small karsts are very dangerous for drilling and therefore it is important to detect them [10]. The main drawback of Logging While Drilling (LWD) tools is related to their investigation area, which is located tens of meters behind the drilling bit and around the tool. Therefore, the information about kartification conditions that can be provided by LWD tools, arrives way too late from the drilling safety point of view [18, 19]. Thus there is no technology that would allow us to *predict* individual karsts or zones of karstification based on direct measurements.

Another approach corresponds to *early detection* of karstification zones based on analysis of real-time drilling data, which was presented in [20]. In this paper it was shown that there are certain patterns in real-time measurements that can be utilized as indicators of karstification processes in the formation. Such indicators can be drilling breaks, step changes in mud losses profile, breccia type of cuttings. As it was shown in [20], even though these events may not cause drilling challenges, their detection can serve as an indicator of a zone with geological conditions favorable to karstification and thus of an increased likelihood of encountering karsts while drilling.

Manual detection of these events through the corresponding patterns in the real-time drilling data may not be feasible as it requires operator presence and attention 24/7. It may also be challenging as patterns in drilling data are usually masked by noise and thus can be missed or misinterpreted. To address this challenge, in this paper we propose an algorithm that automatically detects suspicious changes in the drilling data that may correspond to these events of interest. It attracts attention to these intervals, and the engineer can then analyze them closer to confirm that they indeed correspond to karstification objects.

Detecting frequent events corresponding to karstification objects (and thus the fact that we are drilling through a karstification zone) can be used for decision support, changing of well trajectory, switching to PMCD type of drilling and preparing LCM. Fully automatic detection of karstification objects from drilling data is a very difficult task and can hardly be solved by an automatic algorithm. Therefore we provide a method that supports engineers in this task by automatically marking suspicious periods for further analysis. It should be noted that the same method can be adopted for automatic detection of other drilling events not necessarily related to karsts.

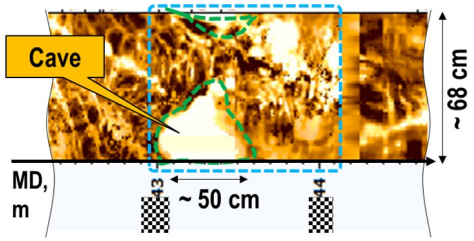

FIGURE 1: BOREHOLE IMAGE OF NOT-COLLAPSED CAVE

The paper is organized as follows. Section 2 introduces karsts and discusses examples of karst-patterns in real-time drilling data. Section 3 explains the concept of the suggested automated event detection method. In section 4 relevant results from the proposed method are presented. Conclusions, discussion and future work are given in Section 5.

2 Karstification patterns

To understand how we can use drilling data to identify zones with high likelihood of karstification, in this section we firstly introduce some important characteristics of karsts and secondly consider real-time drilling measurements which can be used for their detection. We examine data from one of the carbonate fields located in the Barents Sea.

One of the methods to investigate formation characteristics around the wellbore is through borehole imaging. At very shallow depth of investigation we can obtain an image of wellbore walls that can be used to visualize rocks and karsts and define such properties of geological features as height, width, angle and azimuth. In this study, borehole images were used for karst characterisation.

Since many processes contribute to karstification, geometrical properties of karsts vary significantly. Some of the karsts can range from the vug-size small objects, up to the full-cave size. In our case, with borehole images analysis of the entire field in the Barents Sea region, we can conclude that the average vertical size of the caves in this region is up to 2 meters. An example of such a cave is shown in Fig. 1, with dimentions, according to the borehole image, being height - more than 50 cm (19.7”) and circumference - 21.6 cm (8.5 ” section of the well). Drilling through such caves is dangerous as it can lead to total losses of drilling mud, gas kicks and many other consequences. Drilling through this particular cave led to a total mud loss situation with full well control incident that came into effect. A week was required to take control over the well and manage the total mud losses [11].

However, not all caves are open and, generally, after a certain size limit is reached, the cave starts to collapse. Products of cave collapse are known as breccias and are defined as angular fragments of rocks cemented together. An example of collapsed

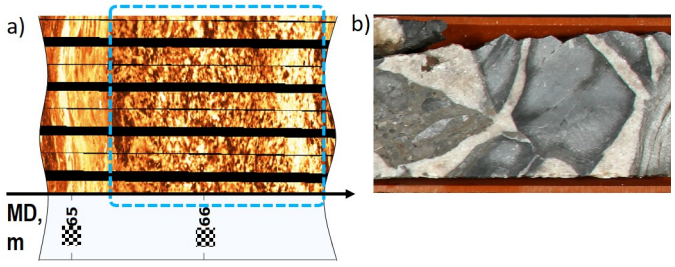

FIGURE 2: a) BOREHOLE IMAGE OF CAVE COLLAPSE BRECCIA. b) CORE SAMPLE PHOTO OF BRECCIA

cave breccia created by evaporite dissolution is presented in Fig. 2. There are many other geological signs of karstfication, but their discussion lies outside the scope of this paper.

Despite the fact that borehole imaging can provide a high resolution data to characterize wellbore rock texture including karsts, borehole images can only investigate the region located tens of meters behind the drilling bit. Thus borehole images are unsuitable for real-time karst detection. At the same time, the identification of karsts and signs of karstification is possible based on real-time drilling and mud loss data. This approach, described in [20], is based on analysis of patterns of real-time data corresponding to karstification objects.

Before describing these patterns, we review the real-time measurements that can be used for karst detection while drilling. Real-time measurements typically can be divided into surface and downhole data (along-the-drillstring measurements are not considered in this paper).

The surface set of measurements consists of: 1) distance drilled per period of time (Rate Of Penetration) 2) the weight on the hook (Hookload) 3) frictional pressure drop along the drilling components in hydraulic circuit (Stand Pipe Pressure). More information about these measurements can be found in [21–23].

Along with the drilling dynamic data, mudflow measurements should be considered to increase the accuracy of karst detection. In some cases, when we cannot detect karsts based on the BHA dynamic data, we can still detect them based on the analysis of mud losses. As shown in paper [20], intervals of vugs are characterized by moderate mud losses, without significant changes, while in bigger caves we can observe a step change of the delta flow profile. So, analysis of mudflow data can complement drillstring measurements. Two examples of the discussed indicators are given below.

Drilling mechanic measurements in the interval of karstification are shown in Figure 3. In this figure we can notice recurring mud losses events at some distance from the cave marked with the arrow #1. Small blue arrows indicate decreases of mud tank volume. From the borehole image study of this interval, it was confirmed that these mud losses were related to drilling through vugs. Total losses were seen after drilling bit entered into a cave

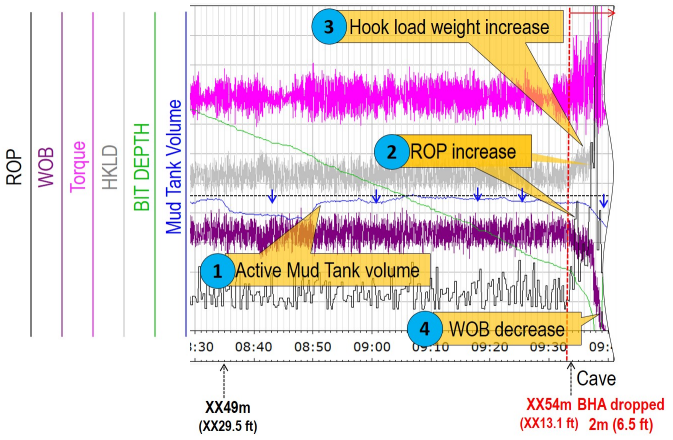

FIGURE 3: DRILLING THROUGH AN INTERVAL OF VUGS AND CAVE

at 09:34 marked with an arrow in the figure. This demonstrates that detecting (minor) mud losses when drilling in carbonates is important as as they can be related to drilling through karstification objects. They can, as in this example, be an early warning signal before drilling into a big cave leading to significant drilling challenges.

When it comes to drilling mechanic measurements, the drilling regime remains constant throughout this interval. However, we can clearly see a rapid increase of ROP(arrow#2) and hookload weight (arrow#3) with a simultaneous drop of Weight On Bit (WOB). This response observed in real-time drilling data can be interpreted as a drilling break resulting from drilling into an open karstic cave. The interval above the cave (based on core sample data) is presented by a weakly cemented rock. Due to significant drop of wellbore pressure (when total losses occur at 09:34) and high stress concentration around the cave the wellbore started to collapse when the stress concentration exceed the rock strength. This example supports the hypothesis that drilling breaks and recurring mud losses events can indicate that the well path is going through a karstification interval.

It should be emphasized that the probability of detecting vugs using drilling breaks increases with an increase of vugs size. Small vugs may not be big enough to effect the BHA mechanical behavior (an increase of ROP, a decrease of WOB, etc.). Still, small vugs can be detected by mud losses, as even small vugs can be highly permeable to absorb drilling fluid, but not big enough to influence on BHA drilling dynamic (an increase of ROP, a decrease of WOB, etc.). So, in [20] the authors suggest to utilize both the mechanical drilling parameters and the mudflow data for detecting karstification objects like vugs.

The next example demonstrates drilling through an interval of large vugs, probably formed due to post-depositional (e.g. karstic) carbonate dissolution. As shown in Figure 4, entering in

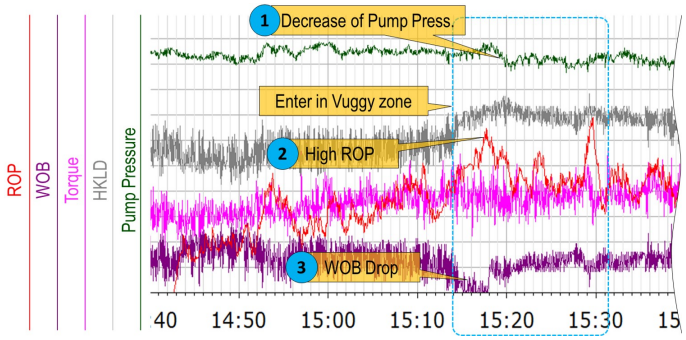

FIGURE 4: DRILLING THROUGH THE INTERVAL OF VUGS

a zone of vugs is also accompanied by a drilling break (high ROP - arrow #2 and WOB drop - arrow #3). Here we can also observe a decrease of Pump Pressure linked with losses of drilling mud into conductive patches.

In this paper, we focus on the most reliable indicators of karsts, which are drilling breaks and mud losses profile. Step-changes of delta flow profile, can be related to drilling through highly conductive karsts, or small fluctuations of delta flow, can often be linked with a smaller karstification objects. To detect drilling breaks we need to detect instances where ROP significantly increases with a decrease of WOB. In both cases, we need to detect a point of change in the corresponding time series and classify whether this change is the one we are looking for (e.g. the onset of reduction in delta flow with sufficiently high total losses after that point, or a sufficiently high increase of ROP).

Detection of karstification-related patterns in the drilling data requires that other possible factors affecting drilling and mud circulation remain constant. In the scope of this study we select/consider periods of data with other drilling parameters being constant.

3 ADAPTIVE DIFFERENTIATING FILTER (ADF)

One of the main challenges in analyzing drilling data is that important information is usually masked with noise. It is common to utilize some kind of filtering to eliminate or reduce the noise in the measured signal. While there are various filters that can be applied to filter out the noise [24–26], one common characteristic of many of them is what can be called a window size. It tells how many data points are effectively used in calculating the filtered value. For example, for the moving average filter, this will be the size of the sliding window involved in averaging. The proposed filter is a modification of the filter described in [27].

The window size of a filter affects both the noise and the original signal. The higher is the window size, the better are the noise attenuation properties of the filter. At the same time, the window size used in averaging/filtering also affects the original signal: large window size results in filtering out fast variations of the signal, keeping only its slowly-varying components. Depending on the selected window size, the filter can have very good noise attenuation properties, but bad performance in capturing fast changes in the signal (for large window sizes); or it can very well capture fast changes in the signal, but have low noise filtering properties (for small window sizes). The former one cancels the noise, but wipes out information from the signal. The later keeps the information, but does not unmask it from the noise. One should therefore choose the window size depending on the properties of the signal and the noise. Signals significantly change during drilling and for some instances one needs a filter with a large window to capture small/slow changes in the signal, while in other cases one needs a small window to accurately capture fast signal changes. This can be achieved by using several filters and switching between them based on the user's judgment. This is not convenient, as it requires experience and multiple actions from the user, as well as introduces an additional human factor in processing and analyzing the data.

In this section we propose an adaptive differentiating filter that automatically adjusts the size of the window to achieve maximal allowable filtering while preserving desired accuracy in capturing fast changes in the signal (as will be explained below). The filter increases the window size when the noisy signal is slowly varying and thus high-level filtering is needed to capture these small slow changes. It automatically decreases the window when the signal is quickly varying and it is more important to capture these fast changes since the effect of noise becomes less important. In addition to that, the filter estimates the derivative of the signal, which is quite often very important in detecting and classifying various events from time series. Optimal filtering provided by the filter is especially helpful here, as the numerical calculation of derivatives is especially sensitive to measurement noise.

To present the filter, we consider a sequence of time instances t_i and the corresponding measurements $y_i, i = 1,...N$. The measurement consists of the true signal $\bar{y}_i$ and noise m_i.

$$y_i = \bar{y}_i + m_i \tag{1}$$

We assume that m_i has zero mean.

The adaptive differentiating filter consists of two operations conducted recursively: 1) signal and derivative estimation (given a window) and 2) window adaptation.

1) Signal and derivative estimation: For a time instant t^*, we define a window centered at t^* and having a radius WR as the sequence of instances $W = [t_i : \ i = *-WR, *+WR]$, where $*$ corresponds to the index of t^*. To find an estimate of $\bar{y}(t^*)$ and its derivative $d\bar{y}/dt(t^*)$, from the data given in window W, we calculate the estimate of the signal $\bar{y}(t^*)$ and its derivative $d\bar{y}/dt(t^*)$ by solving the least-squares fit problem:

$$\sum_{t_i \in WR} |y(t) - (k(t_i - t^*) + b)|^2 \to \min_{k,b}. \quad (2)$$

Then,

$$\hat{y}(t^*) = b \quad (3)$$

$$d\hat{y}/dt(t^*) = k, \quad (4)$$

where $\hat{y}(t^*)$ and $d\hat{y}/dt(t^*)$, are the estimates of $\bar{y}(t^*)$ and $d\bar{y}/dt(t^*)$.

2) Window adaptation: at this step we check the accuracy of how the straight-line segment $\hat{y}(t) = k(t - t^*) + b$ approximates the data series over the window W. If

$$(\max_{t_i \in WR} |k(t_i - t^*) + b - y(t_i)| > \delta) \quad \& \quad (WR > WR_{min}), \quad (5)$$

i.e. if $\hat{y}(t)$ does not fit $y(t)$ over the window W with the required accuracy δ (which is a design parameter of the filter) and the window radius can be reduced without violating the lower limit for the window radius WR_{min} (specified by the user), then the window radius is reduced, the linear fit function is recalculated, and the condition (5) is checked again. This is repeated until either the accuracy requirement is met or the window radius has reached the minimal value WR_{min}. This process is illustrated in Figure 5.

If

$$(\max_{t_i \in WR} |k(t_i - t^*) + b - y(t_i)| < \delta) \quad \& \quad (WR < WR_{max}), \quad (6)$$

i.e. $\hat{y}(t)$ approximates the $y(t)$ over the window W with the desired accuracy, and window radius can be increased without violating the upper limit for windoe radius WR_{max} (specified by the user), then the window radius is increased, the linear fit function is recalculated until and the condition (6) is checked again. This process is repeated until it is not possible to increase the window radius without either violating the accuracy of approximation or exceeding the upper limit WR_{max}. This process is demonstrated by Figure 6.

The output of the algorithm at this stage is the estimate of the signal and its derivative at time instant t^* and the maximal window radius WR^* reached in the window adaptation process. For the next time instant t^*, the initial window radius is taken as the largest window radius WR^* from the previous step. This significantly speeds up the calculation.

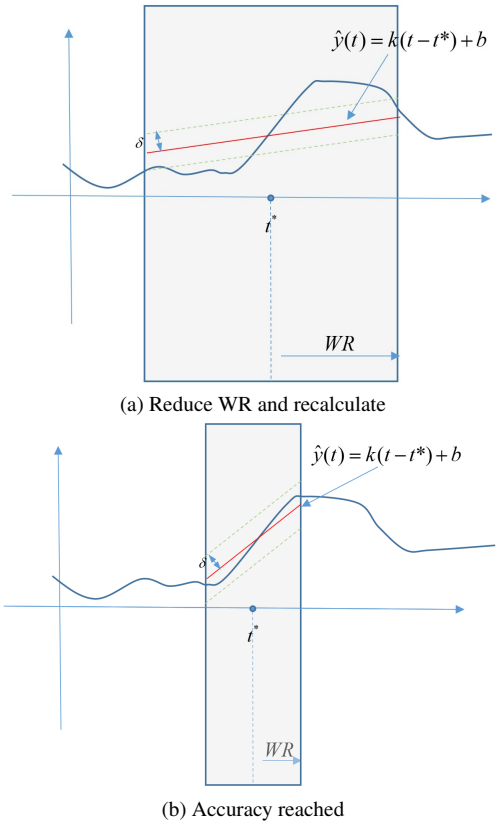

FIGURE 5: Window adaptation from a too large window radius (a) to new window radius where the accuracy is reached (b)

To summarize, the algorithm takes parameters WR_{min}, WR_{max} and δ as inputs and processes the data series t_i, y_i to output estimates of the signal $\bar{y}(t_i)$ and its derivative $d\bar{y}/dt(t_i)$ as well as the radius of the maximal window WR^* corresponding to these estimates.

Parameter WR_{min} determines the minimal level of filtering, as the window radius will always be larger than or equal to WR_{min}. Parameter WR_{max} determines the maximal level of filtering, as the window radius will always be less than or equal to WR_{max}. Parameter δ must be chosen such that the noise m_i in equation (1) satisfies $|m_i| < \delta$ for all i. In practice this parameter is either known or can be estimated from the data. The closer δ to the actual limit on the noise, the more accurate is the filter for the given WR_{min} and WR_{max}.

Performance of the filter is demonstrated in Figure 7 for the case of ROP. In the presented interval, high values of ROP are related to drilling into open karsts leading to BHA drops (spikes in ROP). To capture this behavior, ROP is calculated from the Bit Depth signal with the ADF filter (as a time derivative of the Bit

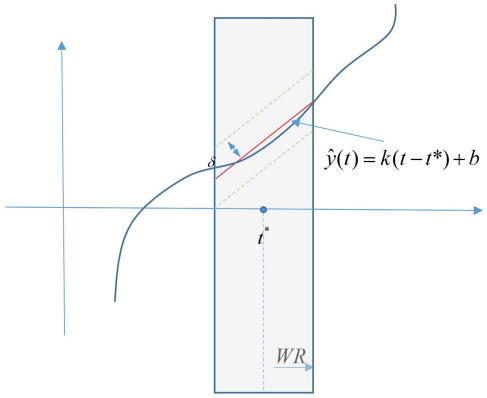

(a) Increase WR and recalculate

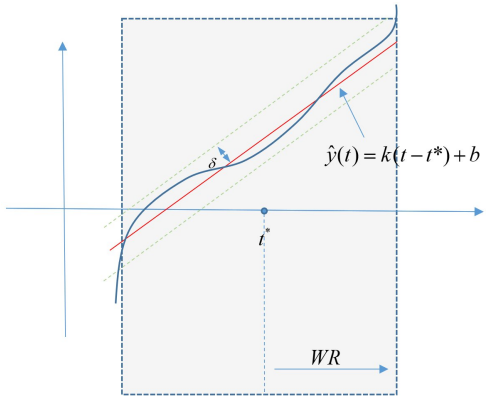

(b) Maximal window radius with feasible approximation is reached

FIGURE 6: Window adaptation starting from window radius where the desired accuracy of the linear approximation is satisfied (a), to a maximal window radius having the desired accuracy (b).

Depth). It can be seen that the window radius is minimal when the signal experiences relatively fast changes. The small window radius can be used as a flag indicating changes for detection of drilling events, as, for example, in detection of drilling breaks and mud losses corresponding to karstification objects.

In Figure 7 we also show a comparison between Gaussian filtering of the ROP data and ADF filter. As illustrated in the figure, the result of Gaussian filtering method with fixed parameters (shown in blue line) provides good filtering of the slowly varying part of the ROP signal, but fails to properly capture the ROP spike (as shown in the zoomed window). The ADF filter (green line) is adjusted automatically to keep the behavior of initial signal (grey line). An overall view on the entire interval shows that both main trends and high-amplitude changes in measurements are successfully captured by the ADF algorithm. This is an important property of the ADF algorithm for applications to real-time measurements analysis when we need to capture both,

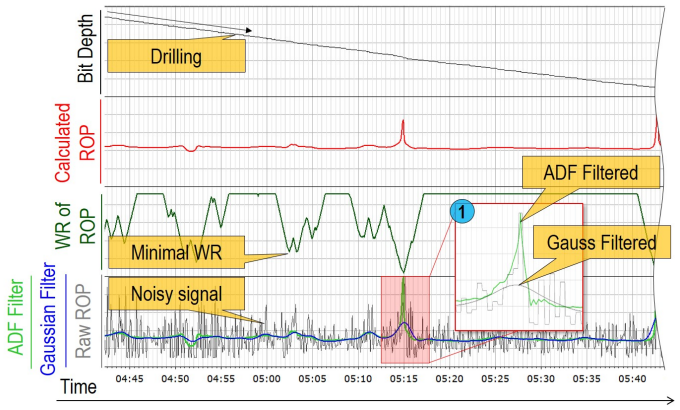

FIGURE 7: ADF algorithm implementation on filtering raw drilling data - ROP

small/slow and large/fast changes in the data.

3.1 Windows radius for events detection

The adaptive window radius provides an effective and accurate indication of variations in the time series. As the accuracy of the approximation must be guaranteed, the adaptive window is forced to drop whenever it encounters rapid or large changes in the data signal where the linear polynomial no longer fits the data. By utilizing an appropriate δ value as a threshold for window adaptation, abnormalities in the data may be discovered from a drop in the window radius below a defined threshold. This concept can be taken advantage of to detect changes in the drilling data for event detection.

3.2 Pseudo-Code

Below, the workflow of the algorithm is described briefly in the form of pseudo-code.

Algorithm for: Adaptive Differentiating Filter

Data: Raw measurements signal
Result: filtered signal, its derivative estimate and the radius of the maximal window
while *data in stream* **do**

1. Use current window radius around current time instant
2. Calculate least squares fit regression estimate over the window
3. Perform window adaption from accuracy check
   if accuracy is not met, reduce window radius and recalculate until accuracy or minimum window reached
   if accuracy sufficient, increase window radius and recalculate while the desired accuracy (specified by δ) is maintained and the window radius is below WR_{max}
4. Utilize the already found optimal window radius for the next time instant

end

4 CASE STUDY - AUTOMATED DETECTION OF KARSTS AND FRACTURES

The following section presents results from a case study on automated karst events detection using adaptive differentiating filter. Here we apply ADF to the set of drilling data containing intervals that the operator company reported as containing fractures, vugs and caves.

Figure 8 presents a complete set of data, both raw and processed, corresponding to the selected interval. The first track (from top to bottom) displays the borehole image with marked intervals of open fractures, vugs and cave in depth-domain. The second track - "drilling data", displays a typical set of surface and downhole measurements in time-domain such as Torque, Pump Pressure, ROP, delta flow, hookload - the weight on the hook to control the weight applying on the bit (WOB) and downhole WOB measurements. These raw measurements are given to provide an overview of drilling within the discussed interval. Tracks marked with letters a to f represent certain outputs of the ADF algorithm used to detect events related to karstification objects.

Five time intervals will be considered as illustrated in the figure (Events 1 to 5). The sections identified as open fractures are intervals where the operator company encountered mud loss situations. They are marked as Events 1, 2 and 4. Event 3 is interpreted as vug interval. Event 5 illustrates cavity of more than 50 cm in length with circumference of 21.6 cm. These intervals are highlighted in blue, denoting the start and stop time of each event. These benchmark intervals will serve for validation and evaluation of the ADF algorithm that automatically detects changes in drilling data related to drilling breaks and mud losses.

In this example, drilling was performed with managed pressure drilling system using a subsea module pump equipped with high-precision sensors of mudflow rate. The measured flow rate can give indications of loss zones, so the calculated delta flow is utilized as one of the inputs for testing ADF for automated event detection. Drilling breaks within carbonate intervals can often indicate that the well trajectory encounters a karstification object. Thus, we utilize sudden drops in WOB and surges in ROP (drilling break pattern) as an indication of a karstification object and capture these changes with the ADF filter.

Let us now consider an application of ADF algorithm for drilling events detection based on three inputs: WOB, ROP and delta flow, as demonstrated in Figure 8. The hypothesis of event detection in the ADF algorithm is that the window radius experiences a minimal value when the signal and its derivative experience rapid changes. The corresponding minima of the window radius are marked with stars. Changes of the window radius for the given inputs are displayed in tracks *b*, *d* and *f*. Another consideration which can be used for events detection is the rate of change of the measurements. As was discussed earlier, it is expected to observe a relatively sharp change in delta flow profile when the well path crosses cave. A similar behavior is fair for WOB and ROP measurements. For open fractures (fractures with mud losses) the rate of change of the discussed measurements is different from caves. Moreover, it is often the case that open fractures are detected only by delta flow measurements and not by ROP or WOB changes as some of the fractures can be relatively small and might not affect the dynamics of the BHA.

For events 1, 2 and 4, benchmarked as open fractures we can notice that the calculated rate of change of the delta flow drops significantly compared to the average level, indicating mud loss situations with sharp drops in the delta flow. For events 3 and 5, which are benchmarked as karst features of different sizes, WR of delta flow clearly indicates the interval of cave (event 5), the detected mud losses (negative values in track e) did not have any sharp changes in the delta flow, as indicated in no reduction of WR in track f. For WOB (track b) and ROP (track d) inputs, WR reaches its minimum in the intervals 2, 3 and 5, indicating quick changes in these parameters.

The main value of the discussed approach in the context of drilling events detection is that it simplifies the process of the detection of suspicious changes in drilling data. For example, it can not be clearly seen from the raw drilling data (shown in the track "drilling data") that some events were occurring. While the visual analysis of WR and the calculated signal derivatives can easily indicate that there are changes in drilling data that might be linked either with regular drilling instances or with drilling through karsts.

In this section we have demonstrated that the ADF algorithm is capable to reveal events in complex datasets such as real-time drilling measurements. Validation of event detection hypothesis showed the potential for online karst patterns detection from different real-time input signals such as delta flow, WOB and ROP.

From the presented case study we can see that the ADF algorithm applied to WOB, ROP and delta flow measurements successfully detects five out of five benchmark intervals corresponding to fractures or karsts. This detection occurred using either one, two or all three measurements. From the results, it is clear that the ADF can be utilized to detect karsts and fractures whenever they cause rapid changes in a measurement or its rate of change.

For online drilling event detection, the ADF is robust and reliable, as it is efficient in approximation and detection and applicable to various datasets. This algorithm is highly modular, easy to tune and it can provide reliable results that match with variations that can also be observed.

5 CONCLUSIONS

In this paper, we propose an algorithm, called adaptive differential filter, that can be utilized for automated detection of patterns in real-time drilling data corresponding to karstification objects. The adaptive differential filter automatically detects step changes in the delta flow as well as instances corresponding to drill breaks. Both can correspond to encountering karstification objects while drilling in carbonates.

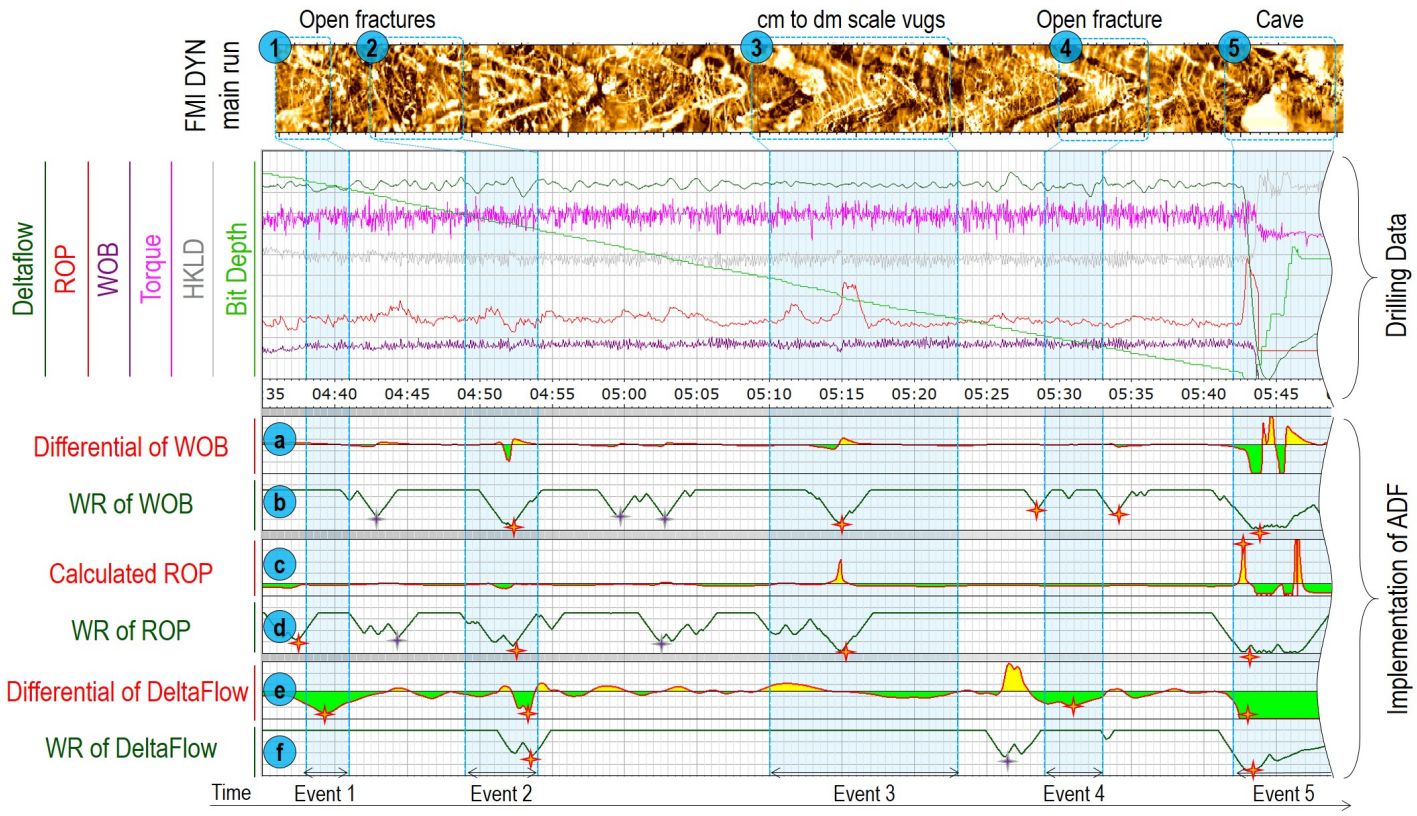

FIGURE 8: ADF algorithm implementation on drilling data

Based on a case-study corresponding to drilling in carbonates in a field in the Barents sea, it can be concluded that the proposed algorithm demonstrates good results for automated event detection and can efficiently locate change points in measurements corresponding to fractures, vugs, caves and possibly other karst-related events with high precision.

It is the engineer's responsibility to further investigate and evaluate the changes in data indicated by the algorithm, taking into account the totality of available information. In this way, the final responsibility is still on the engineer, while the proposed automatic algorithm helps the engineer to detect karstification objects and zones.

Future work includes incorporating multiple inputs for increasing reliability and confidence of karsts patterns and other drilling events detection, as well as reducing the number of potential false alarms. This will contribute to automation of karsts and other events detection to a higher degree and help with more consistent classification of complex real-time drilling data. Research results presented in this paper also contribute to digitalization and automation of today's manual interpretation of drilling measurements for detecting drilling events while drilling.

ACKNOWLEDGMENT

This research is a part of BRU21 – NTNU Research and Innovation Program in Digital and Automation Solutions for the Oil and Gas Industry (www.ntnu.edu/bru21) and supported by Lundin Norway AS. The authors are grateful to Per Haugum and Bård Fjellså from Lundin Norway AS, for their decisive technical contributions in important stages of this research.

REFERENCES

[1] Joshi, R. M., and Singh, K. H., 2020. "Carbonate reservoirs: Recent large to giant carbonate discoveries around the world and how they are shaping the carbonate reservoir landscape". In Petro-physics and Rock Physics of Carbonate Reservoirs, Springer Singapore, pp. 3–14.

[2] Laouafa, F., Guo, J., and Quintard, M., 2019. "Underground rock dissolution and geomechanical issues". In 53rd US Rock Mechanics / Geomechanics Symposium ARMA 19, ARMA, pp. 1–12.

[3] Nicod, J., 2003. "A little contribution to the karst terminology: Special or aberrant cases of poljes?". *Acta Carsologica,* ***32***(2), May, pp. 29–39.

[4] Gawor, L., and Jonczy, I., 2014. "Surface karst landforms of the Notranjska region (south-western Slovenia)". *Geo-*

tourism/Geoturystyka, ***37***, Feb, pp. 55–60.

[5] Bella, P., 1998. "Genetic types of caves in Slovakia". *Acta Carsologica,* ***27***(2), July, pp. 15–23.

[6] Peng, C., Dai, J., and Yang, S., 2013. "Seismic guided drilling: Near real time 3D updating of subsurface images and pore pressure model". In International Petroleum Technology Conference, International Petroleum Technology Conference, pp. 1–6.

[7] Terwogt, J., Makiaho, L., van Beelen, N., Gedge, B., and Jenkins, J., 2005. "Pressured Mud Cap Drilling from a semi-submersible drilling rig". In SPE/IADC Drilling Conference, Society of Petroleum Engineers, pp. 1–6.

[8] Niznik, M. R., Elks, W. C., and Zeilinger, S. C., 2009. "Pressurized mud cap drilling in Qatar's North Field". In IADC/SPE Managed Pressure Drilling and Underbalanced Operations Conference & Exhibition, Society of Petroleum Engineers, pp. 1–11.

[9] Bysveen, J., Fossli, B., Stenshorne, P. C., Skargaard, G., and Hollman, L., 2017. "Planning of an MPD and Controlled Mud Cap Drilling Operation in the Barents Sea using the CML technology". In IADC/SPE Managed Pressure Drilling & Underbalanced Operations Conference & Exhibition, Society of Petroleum Engineers, pp. 1–14.

[10] Claudey, E., Fossli, B., Elahifar, B., Qiang, Z., Olsen, M., and Mo, J., 2018. "Experience using managed pressure cementing techniques with riserless mud recovery and controlled mud level in the Barents Sea". In SPE Norway One Day Seminar, Society of Petroleum Engineers, pp. 1–18.

[11] Tangen, G. I., Smaaskjaer, G., Bergseth, E., Clark, A., Fossli, B., Claudey, E., and Qiang, Z., 2019. "Experience from drilling a horizontal well in a naturally fractured and karstified carbonate reservoir in the Barents Sea using a CML MPD system". In IADC/SPE Managed Pressure Drilling and Underbalanced Operations Conference and Exhibition, Society of Petroleum Engineers, pp. 1–19.

[12] Muir, K., 2006. "MPD techniques address problems in drilling Southeast Asia's fractured carbonate structures.". In International Association of Drilling Contractors, Drilling Contractor, pp. 34–36.

[13] Houng, N. H., Rubianto, I., Abuelaish, A. R., and Abdullah, M. A. B., 2016. "Successful pmcd application significantly improved drilling efficiency on carbonate drilling". In IADC/SPE Asia Pacific Drilling Technology Conference, Society of Petroleum Engineers, pp. 12–.

[14] Jayah, M. N., A Aziz, I. A., Mathews, T., Rojas, F., and Voshall, A., 2013. "Implementation of PMCD to Explore Carbonate Reservoirs from Semi-Submersible Rigs in Malaysia results in Safe and Economical Drilling Operations". In SPE/IADC Drilling Conference, Society of Petroleum Engineers, pp. 1–15.

[15] Amanbayev, Y., and Karmanov, K., 2018. "Successful Implementation of PMCD Technology in Kazakhstan". In SPE Russian Petroleum Technology Conference, Society of Petroleum Engineers, pp. 1–10.

[16] Godhavn, J.-M., Hauge, E., Molde, D. O., Kjosnes, I., Gaassand, S., Fossli, S. B., and Stave, R., 2014. "ECD Management Toolbox for Floating Drilling Units". In Offshore Technology Conference, Offshore Technology Conference, pp. 1–23.

[17] Wang, N., Xie, X.-B., Duan, M.-C., Li, D., and Wu, R.-S., 2019. "Improving seismic image resolution in a carbonate fracture cave region: A case study". In SEG International Exposition and Annual Meeting, Society of Exploration Geophysicists, pp. 1–5.

[18] Maia, W., Rubio, R., Junior, F., Haldorsen, J., Guerra, R., and Dominguez, C., 2006. "First Borehole Acoustic Reflection Survey mapping a deepwater turbidite sand". *Seg Technical Program Expanded Abstracts,* ***25***, Jan, pp. 87–92.

[19] Wu, P. T., Lovell, J. R., Clark, B., Bonner, S. D., and Tabanou, J. R., 1999. "Dielectric-independent 2-mhz propagation resistivities". In SPE Annual Technical Conference and Exhibition, Society of Petroleum Engineers, pp. 1–19.

[20] Maksimov, D., Pavlov, A., and Sangesland, S., 2020. "Drilling in karstified carbonates: Early risk detection technique". In ASME 2020 39th International Conference on Ocean, Offshore and Arctic Engineering, Vol. 11, pp. 1–10.

[21] Macpherson, J., Mason, J., and Kingman, J., 1993. "Surface measurement and analysis of drillstring vibrations while drilling". In SPE/IADC Drilling Conference, Society of Petroleum Engineers, pp. 1–11.

[22] Kirkman, M., 1994. "Use of Surface Measurement of Drillstring vibrations to improve drilling performance". In 14th World Petroleum Congress, World Petroleum Congress, pp. 1–4.

[23] Wylie, R., Soukup, I., Mata, H., Cuff, S., and Ho, A., 2015. "The drilling optimization benefits of direct drillstring surface measurements – case studies from field operations". In SPE/IADC Drilling Conference and Exhibition, Society of Petroleum Engineers, pp. 1–28.

[24] Ralaivola, L., and d'Alche Buc, F., 2005. "Time series filtering, smoothing and learning using the kernel kalman filter". In Proceedings. 2005 IEEE International Joint Conference on Neural Networks, 2005., Vol. 3, pp. 1449–1454.

[25] Babu, C. N., and Reddy, B. E., 2014. "A moving-average filter based hybrid arima and ann model for forecasting time series data". *Applied Soft Computing,* ***23***, pp. 27–38.

[26] Gui, M.-W., 2008. "The basics of noise detection and filtering for borehole drilling data". *The Open Civil Engineering Journal,* ***2***, Sep, pp. 1–10.

[27] Sharifi, F., Hayward, V., and Chen, C.-S., 2000. "Discrete-time adaptive windowing for velocity estimation". *Control Systems Technology, IEEE Transactions on,* ***8***, Dec., pp. 1003–1009.